Materials Research, Vol. 10, No. 1, 5-10, 2007

Magnesium and its Alloys as Degradable Biomaterials. Corrosion Studies Using Potentiodynamic and EIS Electrochemical Techniques

*Wolf Dieter Müller[a], Maria Lucia Nascimento[b], Miriam Zeddies[e], Mariana Córsico[c,d], Liliana Mabel Gassa[c,d], Mónica Alicia Fernández Lorenzo de Mele[c,d]**

[a] *"Charité" Universitätsmedizin Berlin, 10117 Berlin, Germany*
[b] *Technical University of Berlin, 10623 Berlin, Germany*
[c] *Instituto de Investigaciones Fisiocoquímicas Teóricas y Aplicadas – INIFTA, Facultad de Ingeniería, Universidad Nacional de La Plata – UNLP, Casilla de Correo, 16, Sucursal, 4, 1900 La Plata, Argentina*
[d] *Instituto de Investigaciones Fisiocoquímicas Teóricas y Aplicadas – INIFTA, Diag. 113 y 64. CC 16 Suc. 4 La Plata, Argentina*
[e] *University of Applied Sciences Osnabrueck, Osnabrueck, Germany*

Received: July 31, 2006; Revised: November 7, 2006

Magnesium is potentially useful for orthopaedic and cardiovascular applications. However, the corrosion rate of this metal is so high that its degradation occurs before the end of the healing process. In industrial media the behaviour of several magnesium alloys have been probed to be better than magnesium performance. However, the information related to their corrosion behaviour in biological media is insufficient. The aim of this work is to study the influence of the components of organic fluids on the corrosion behaviour of Mg and AZ31 and LAE442 alloys using potentiodynamic, potentiostatic and EIS techniques. Results showed localized attack in chloride containing media. The breakdown potential decreased when chloride concentration increased. The potential range of the passivation region was extended in the presence of albumin. EIS measurements showed that the corrosion behaviour of the AZ31 was very different from that of LAE442 alloy in chloride solutions.

Keywords: *magnesium alloys, biomaterials, corrosion*

1. Introduction

Magnesium and its alloys are light, biodegradable, biocompatible metals that have promising applications as biomaterials[1-6]. Screws and plates made of magnesium alloys provided stable implant materials that degraded in vivo, eliminating the need for a second operation. Additionally, clinical studies showed good biocompatibility[2,4]. A successful osteointegration with an increased bone mass around the magnesium alloys was reported, probably related to the bone cell activation by magnesium. Mechanical properties such as tensile yield strength and Young´s modulus of magnesium ant its alloys are better than those of polymeric implant materials. Particularly, their high strength to weight ratio make them extremely attractive for in vivo applications[3-5]. However, a great deal is still necessary to know the possibilities of magnesium and its alloys in relation to their corrosion susceptibility. Corrosion evaluation in industrial environments shows that dissolution rate of these metals is strongly dependent on the alloy composition and on the corrosive characteristics of the environment[7-16]. However, only a few research works have been published related to their corrosion behaviour in biological media[3,4,6]. The aim of this work is to study the influence of the electrolyte composition on the corrosion behaviour of Mg and AZ31 and LAE442 alloys using potentiodynamic, potentiostatic and EIS techniques.

2. Materials and Methods

Two types of electrochemical cells were used in the experiments: a) a conventional three electrode electrochemical cell, and b) a mini cell system (MCS).

A conventional electrochemical cell with a platinum counter-electrode and saturated calomel (SCE) as reference electrode, coupled to a potentiostat (EI 1286, Schlumberger), with a interface connecting to a personal computer driven by the software Corrware for Windows, was used. The working electrode was included in an epoxi resin giving an exposed area of 1 cm^2. A mini cell system (MCS) was also employed to study different sites of the surface of the same working electrode taking advantage of its suitable design. The MCS is a one-compartment cell which includes the reference and the counter-electrode and ends with a changeable tip (Figure 1). This tip is open at the bottom by which the contact with the working electrode is made (0.8 mm^2 contact area). The system is filled with the electrolyte through a lateral access, using a syringe. All reported potential values are referred to the standard SCE. Pure magnesium (99.98%), LAE 442 (89.6% Mg, 4.0% Li, 3.9% Al, 2.2% Se, 0.2% Mn) and AZ31(96.4% Mg, 2.4% Al, 0.8% Zn, 0.4% Mn, 0.1% Si) rods were used as working electrodes.

Previous to each measurement, the working electrodes were successively polished up to 1200 grade with emery paper, and then with diamond suspension up to 3 μm, degreased with acetone and rinsed with distilled water.

The following solutions were used as electrolytes: a) NaCl solutions: 0.9 g/L, 5 g/L, 9 g/L, 10 g/L; b) Phosphate buffer solution (PBS): 0.2 g/L KCl, 0.2 g/L KH_2PO_4, 8 g/L NaCl, 1.150 g/L Na_2HPO_4 (anhydrous); c) PBS with the addition of albumin: 0.1 g/L, 1 g/L and 10 g/L.

Single sweep potentiodynamic polarization curves and cyclic voltammograms were performed at 10 mV/s, between – 2.25 V and different anodic limits. The passivation currents and breakdown potentials (E_{bd}) were determined. Open circuit potential was recorded

*e-mail: mmele@inifta.unlp.edu.ar
Article presented at the IV Congresso Latino Americano de Órgãos Artificiais e Biomateriais (COLAOB 2006), August 8 and 11, 2006, Caxambu, MG, Brazil

Figure 1. Mini cell system (MCS) used for electrochemical measurements.

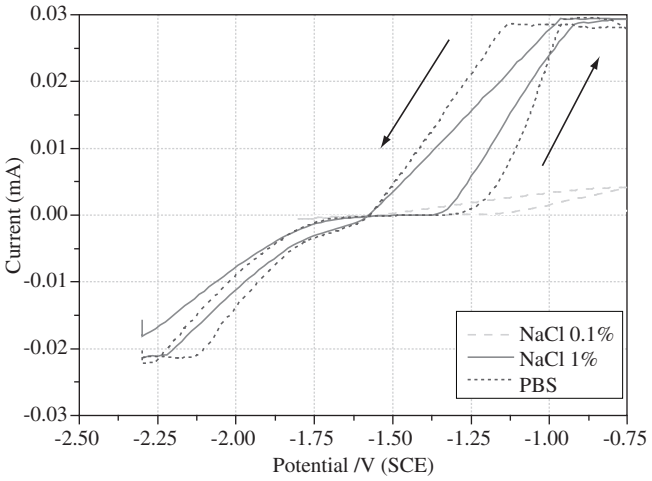

Figure 2. Current *vs.* potential polarization curve of AZ31 magnesium alloy in different electrolytes.

during 5 minutes before each measurement. At least three anodic polarization curves were generated for each condition, although higher amount of measurements were made for Mg because of the scattering values of the corrosion parameters of the pure metal. Transient current during two potential steps (-1.8 V and E ($-0.9 \leq E \leq -1.6$)) were also recorded. EDX and SEM characterizations of the surface were made before and after the electrochemical experiments.

Impedance measurements were carried out using a frequency analyzer, which included a potentiostat (Zahner IM6d). The experiments were conducted by applying a small amplitude perturbation of 5 mV in a sine waveform, and by scanning the modulus of impedance and the phase shift over the frequency range from 1 mHz to 1 MHz. The applied potential range was $-1.7\ V \leq E \leq -1.2\ V$.

3. Results and Discussion

Figure 2 shows the cyclic potential scan made with AZ31 alloy immersed in different chloride-containing solutions. In all cases, a passive region characterized by low current records can be observed during the anodic scan, at potentials higher than -1.7 V. This behaviour could be associated to the formation of a thin metastable, partially protective film[7,8,10,12,13]. The passive regions extends up to the E_{bd} characterized by the abrupt increase of current density[17,18]. At this potential, localized corrosion begins, starting as irregular small pits (Figure 3). Subsequently, the pits spread laterally and cover large areas. Cracks, frequently associated to hydrogen formation during corrosion process could also be observed on the surface. Localized corrosion of magnesium and its alloys in chloride environment has a tendency to be self-limiting and current reaches a constant value in the pitting region, opposite to stainless steel where pitting is autocatalytic[9,11]. The E_{bd} shifted to more cathodic values and the current increased when higher chloride concentrations were used. Larger and deeper pits were formed on the Mg and its alloys surfaces in 9 g/L chloride solutions than at lower concentration. The analysis of corrosion product layer by EDX revealed Mg, Cl and O signals that could be associated to $MgCl_2$, MgO or $Mg(OH)_2$.

If the potential is scanned anodically up to potentials more anodic than E_{bd} and then cathodically (cyclic scan) (Figure 2), it can be observed that current remains high indicating an imperfect passivation. It can be interpreted considering that once pitting began no passivation could be achieved even at very low potential values[17,18].

The pH of organic fluids "in vivo" is usually stable because of the presence of buffers. In Figure 2 a cyclic potential scan made in

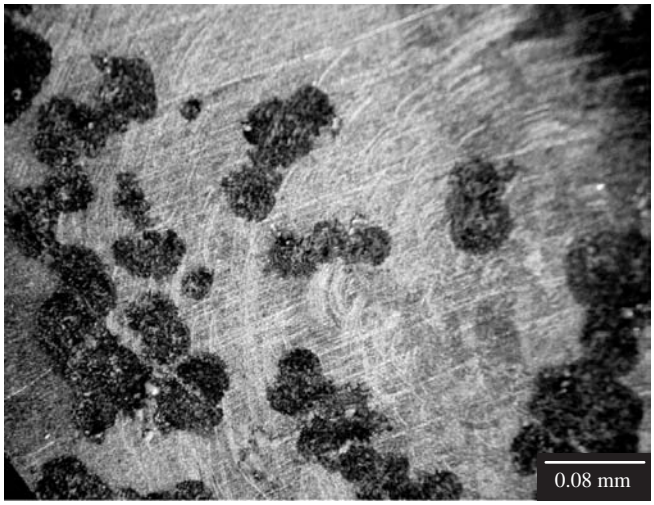

Figure 3. Microphotograph of the magnesium surface after performing the polarization curve in NaCl solution (50x).

PBS is also included. Phosphate buffer renders the surface more protective by controlling the surface pH. Otherwise, concentration of H^+ changes locally by the consumption of hydrogen ions during the corrosion process[9,11]. The difference between E_{bd} and E_{corr} in PBS is higher than that obtained in chloride solutions of similar concentrations but in the absence of phosphate, indicating a larger passivity range in the presence of these ions..

E_{bd} than the plain PBS (Figure 4). Polarization curves made with MCS in different places of a magnesium sample show dissimilar behaviours at the different sites. Both, current and E_{bc} measured with the MCS vary from place to place indicating that the corrosion layer is probably not uniform and does not offer similar protective characteristics.

A SEM microphotograph of a Mg specimen after performing the polarization curve confirms this assumption. An inhomogeneous dehydrated organic film can be observed on the surface. Figure 5 shows the localized attack when albumin is present. Round shape pits smaller than those obtained in the absence of albumin were detected.

The elemental analysis revealed the signals of reduced oxygen and carbon indicating the presence of organic components on the

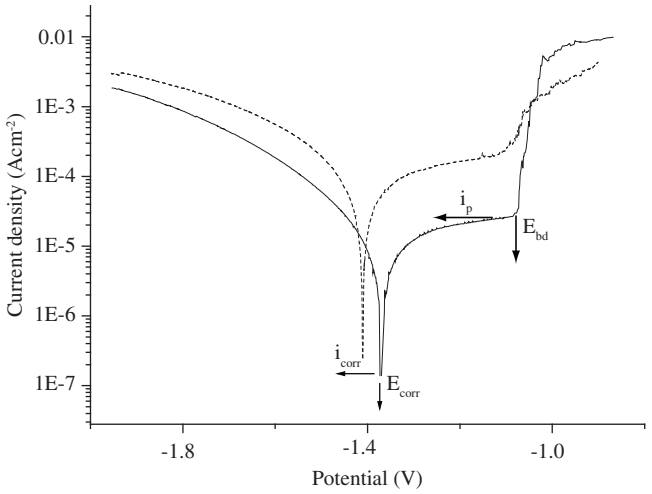

Figure 4. Log i vs. potential polarization curve made in PBS + 0.1 g/L albumin. Passive and corrosion currents (i_p i_{corr}), the breakdown and corrosion potentials (E_{bd}, E_{corr}) are indicated. Dashed line corresponds to the control polarization curve made in PBS.

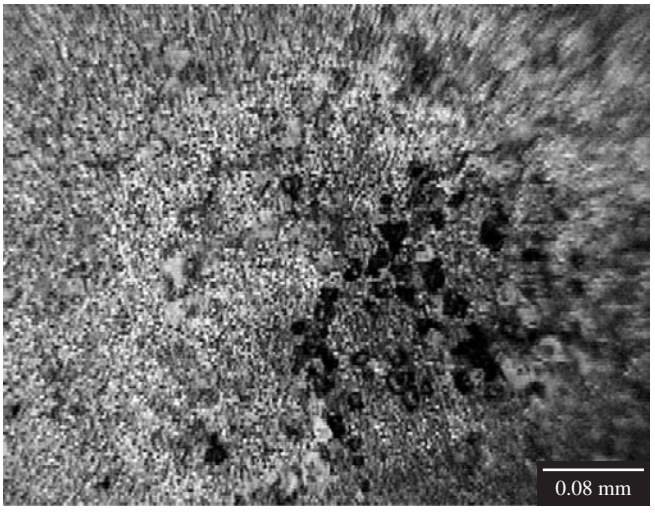

Figure 5. Microphotograph of the magnesium surface after performing the polarization curve in an 0.1%albumin-containing solution (50X). Localized attack with small pits can be observed.

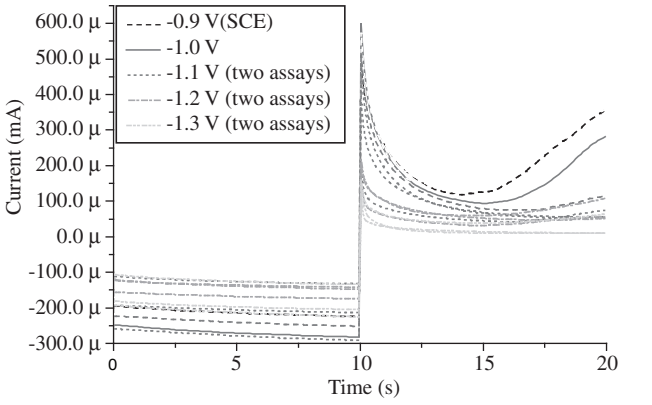

Figure 6. Transient currents corresponding to AZ31 magnesium alloy immersed in 1 g/L NaCl. Different records at -1.8 V are shown (left) followed by a potential step to a potential E in the -1.3 V to -0.9 V potential range (right). At potentials ≥ -1.2 V a current increase is observed.

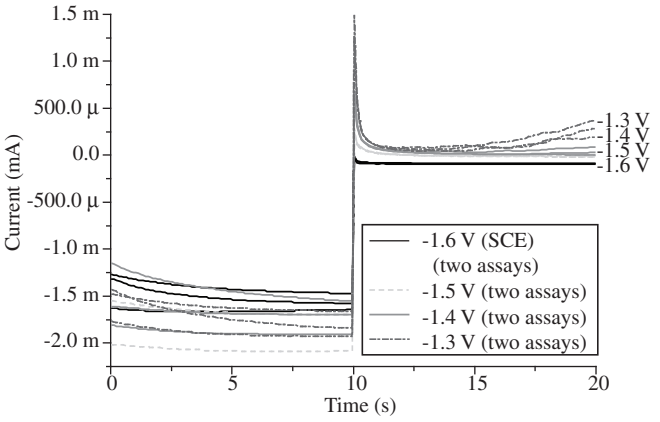

Figure 7. Transient currents corresponding to AZ31 magnesium alloy immersed in 10 g/L NaCl. Different records at -1.8 V are shown (left) followed by a potential step to a potential E in the -1.6 V to -1.3 V potential range (right). At potentials ≥ -1.4 V a current increase is observed.

surface. Protein adsorption is probably involved in the corrosion process[19-21].

Transient currents (Figures 6 and 7) show that after the initial decrease current remains constant at potentials more cathodic than -1.3 V for AZ31 immersed in 1g/L or 10 g/L NaCl respectively. At higher potentials current increased and pits were observed on the surface.

The Nyquist plots of both alloys in NaCl solutions (Figure 8) show only one capacitive contribution associated with the dissolution of the alloy. At low frequencies a not well defined contribution can be observed, probably associated to a pitting process (shown in Figure 3). The shape of the plots of both alloys is similar but the impedance value of the LAE 442 alloy is markedly higher than that of AZ31, at E = -1.6 V. Consequently, metallurgical factors seem to play an important role in the corrosion process of these alloys at this potential in chloride solutions. However, at more anodic potentials, where localized corrosion is taking place, both alloys show that the impedance values diminished drastically independent of the alloy composition.

EIS measurements carried out in PBS (Figure 9), show a new contribution at intermediate and low frequencies with similar impedance values for both alloys. When the plots corresponding to PBS and NaCl solutions are compared, it can be noticed that impedance values are very different in the case of AZ31 alloy. Corrosion process is hindered in phosphate solutions. However, similar impedance values were recorded for LAE442.

The passive region is more clearly defined in the case of magnesium alloys than for pure Mg[9,11]. The formation of Al_2O_3 inner layer may hinder the corrosion process in Al-containing alloys such as LAE442 and AZ31. Corrosion process may also be affected by metallurgical factors, alloying additions and impurities. For AZ31 alloy primary α, eutectic α, and β phases are defined. It has been reported that localized corrosion in chloride solutions concentrates in grain boundaries with selective attack which is followed by undercutting and falling out of grains[7,9,11].

The experimental data can be described by the following transfer function:

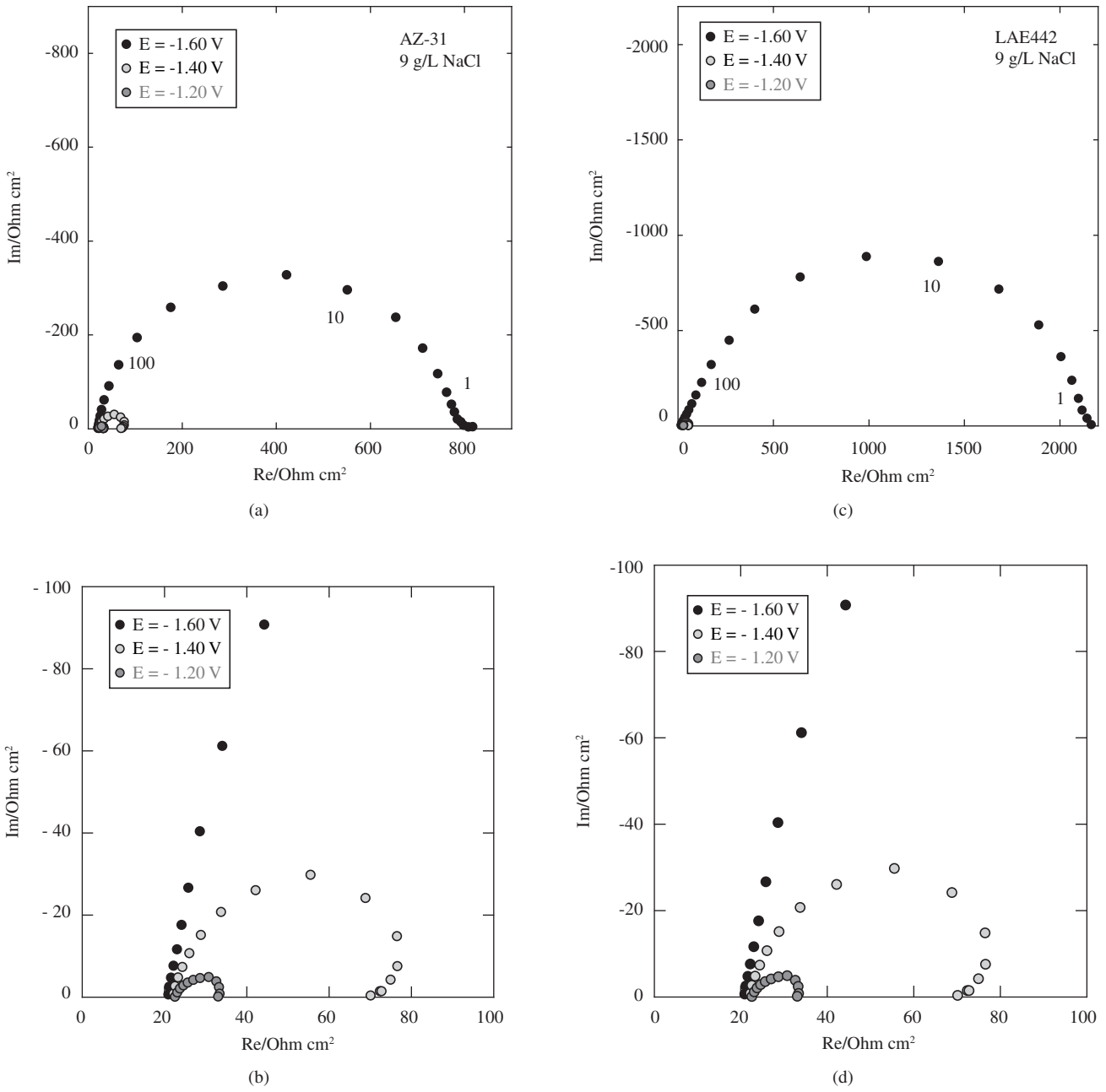

Figure 8. Impedance diagrams of magnesium alloys in 9 g/L NaCl solution at different operational potentials (-1.6 V, -1.4 V, -1.2 V). a) AZ31 alloy; b) Detail at higher magnification; c) LAE442 alloy; and d) Detail at higher magnification.

$$Z_T(j\omega) = R_\Omega + Z \quad (1)$$

$$\text{where } Z^{-1} = [CPE]^{-1} + Z_f^{-1} \quad (2)$$
$$\text{and } \omega = 2\pi f$$

R_Ω, corresponds to the ohmic resistance of the electrolyte, whereas $[CPE] = [C_{dl}(j\omega)\alpha]^{-1}$ involves the double layer capacitance, C_{dl}, and the parameter α, that takes account of the interface roughness. Z_f^{-1} in Equation 2 corresponds to:

$$Z_f^{-1} = (R_{ct} + Z_{ad}) \quad (3)$$

R_{ct} denotes the charge transference resistance and Z_{ad} relates to the second time constant in the case of the PBS results.

There is a good agreement between experimental results and calculated data when the following values are used in the fitting process: $C_{dl} \cong 25 \pm 5\ \mu F\ cm^{-2}$ and α between 0.76 and 0.90. The latter values indicate that the real area of the electrode is greater than the geometric area. The calculated parameters for the second time constant obtained in the PBS could be associated to an adsorption process.

Phosphate could favour the reduction of corrosion susceptibility stabilizing the passive film[22]. It has been reported that phosphate ions adsorb strongly on aluminium oxide hindering the pitting corrosion. The formation of a complex between aluminium and phosphate has been proposed[23,24]. Phosphate adsorption process could also inhibit the aluminium-containing magnesium alloys corrosion, considering that

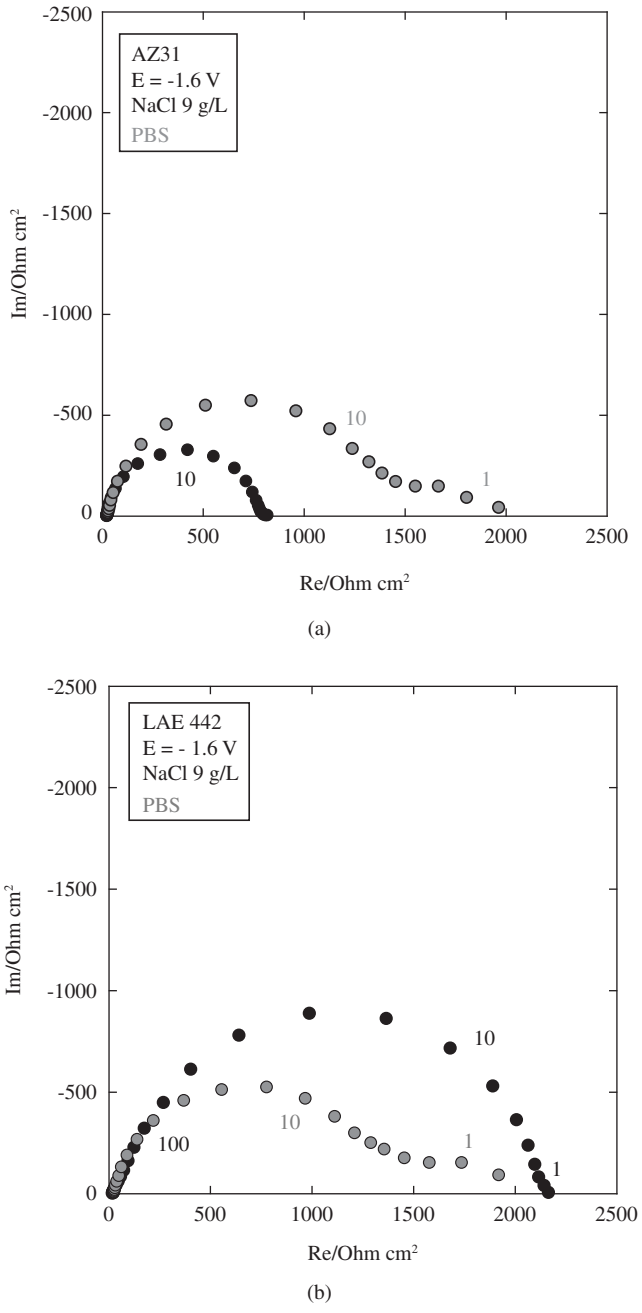

Figure 9. Comparison of impedance results of AZ31 and LAE442 alloys in 9 g/L NaCl solutions and PBS at E = -1.6 V.

the formation of aluminium oxide under the magnesium hydroxide layer has been proposed[9,11]. Phosphate + calcium containing layer was found in vivo on magnesium alloys[3] and CaP base apatite was found after 14 days immersion tests in calcium and phosphate containing solution "in vitro"[3,4]. It is worth mentioning that the buffer capacity may also influence on the corrosion process. It was found that the corrosion rate is higher when the buffer capacity is lower. These data are consistent with the lower corrosion of cast pure magnesium in borate buffer reported previously by Subba Rao et al.[25].

4. Conclusions

Corrosion of Mg and its alloys is localized and is strongly influenced by the concentration of the ions and proteins present in organic fluids. Different electrochemical techniques show that chloride ions favours the metal dissolution and phosphate ions hinder the corrosion attack. Proteins like albumin also inhibit this process. The comparison between AZ31 and LAE442 alloys shows that LAE442 is more resistant to corrosion attack.

Acknowledgment

Authors acknowledge the financial support of UNLP (I095), CONICET (PIP 6075), ANPCyT (PICT 12508-02) and SeCyT-DAAD (Project DA/PA05-SXII/032)

References

1. Heublein B, Rohde R, Kaese V, Niemeyer M, Hartung W, Haverich A. Biocorrosion of magnesium alloys: a new principle in cardiovascular implant technology? *Heart*. 2003; 89:651-659.
2. Zartner P, Cesnjevar R, Singer H, Weyand M. First successful implantation of a biodegradable stent into the left pulmonary artery of a preterm baby. *Catheter Cardiovascular Interview*. 2005; 66:590-594.
3. Witte F, Kaese V, Haferkamp H, Switzer E, Meyer-Linderberg A, Wirth C, Windhagen H. In vivo corrosion of four magnesium alloys and the associated bone response. *Biomaterials*. 2005; 26:3557-3563.
4. Witte F, Fischer J, Nellesen J, Crostack H, Kaese V, Pisch A, Beckmann F, Windhagen H. In vitro and in vivo corrosion measurements of magnesium alloys. *Biomaterials*. 2006; 27:1013-1018.
5. Staiger M, Pietak A, Huadmai J, Dias G. Magnesium and its alloys as orthopaedic biomaterials: a review. *Biomaterials*. 2006; 27:1728-1734.
6. Li L, Gao J, Wang Y. Evaluation of cyto-toxicity and corrosion behavior of alkali-heat-treated magnesium in simulated body fluid. *Surface Coating*. 2006; 185:9-98.
7. Song G, Atrens A., Stjohn D, Nairn J, Li Y. Electrochemical corrosion of pure magnesium in 1 N NaCl. *Corrosion Science*. 1997; 39:855-875.
8. Song G, Atrens A, Wu X, Zhang B. Corrosion behaviour of AZ21, AZ501 and AZ91 in sodium chloride. *Corrosion Science*. 1998; 40:1769-1791.
9. Song G, Bowles A, StJohn D. Corrosion resistance of aged die cast magnesium alloy AZ91D. *Material Science Engineering A*. 2004; 366:74-86.
10. Song G, Atrens A.Corrosion mechanisms of magnesium alloys. *Advance Engineering Materials*. 1999; 1:11-33.
11. Song G, Atrens A. Understanding magnesium corrosion. A framework for improved alloy performance. *Advance Engineering Materials*. 2003; 5:837-858.
12. Song G. Recent progress in corrosion and protection of magnesium alloys. *Advance Engineering Materials*. 2005; 7:563-586.
13. Ambat R, Aung N, Zhou W. Studies on the influence of chloride ion and pH on the corrosion and electrochemical behaviour of AZ91D magnesium alloy. *Journal Applied Electrochemistry*. 2000; 30:865-874.
14. Tunold R, Holtan H, Hägg Berge M-B, Lasson A, Steen-Hansen R. The corrosion of magnesium in aqueous solution containing chloride ions. *Corrosion Sciences*. 1977; 17:353-365.
15. Miller P, Shaw B, Wendt R, Moshier W. Assessing the corrosion resistance of nonequilibrium magnesium-yttrium alloys. *Corrosion*. 1995; 51:922-931.
16. Weber C, Knörschild G, Dick L. The negative-difference effect during the localized corrosion of magnesium and of the AZ91HP alloy. *Journal Brazilian Chemical Society*. 2003; 14:584-593.
17. Kruger J. Fundamental aspects of the corrosion of metallic implants. In: Syrett B and Acharye A, editors. *Proceeding of the ASTM Symposium, 1978; Kansas City, Mo, USA*. Publication ASTM; 1979. p. 107-127.
18. Szklarska-Smialowska Z., editor. *Pitting Corrosion of Metals*. Nace International. Houston; 1986.
19. Endo K. Chemical modification of metallic implant surfaces with biofunctional proteins (Part 2). Corrosion resistance of a chemically modified NiTi alloy. *Dental Materials Journals*. 1995; 14:199-210.

20. Williams D, Askill I, Smith R. Protein adsorption and desorption phenomena on clean metal surfaces. *Journal Biomedical Material Research*. 1985; 19:313-320.

21. Williams R, Williams D. Albuminum adsorption on metal surfaces. *Biomaterials*. 1988; 9:206-212.

22. Aramaki K. The inhibition effect of chromate-free anion inhibitors on corrosion of zinc in aereated 0.5 M NaCl, *Corrosion Science*. 2001; 43:591-604.

23. Hiromoto S, Tsai A, Sumita M, Hanawa T. Effect of chloride ion on the anodic polarization behaviour of the Zr65Al7.5Ni10Cu17.5 amorphous alloy in phosphate buffered solution. *Corrosion Science*. 2000; 42:1651-1660.

24. Nèmeth Z, Gàncs L, Gèmes G, Kolics A. pH dependence of phosphate sorption on aluminium. *Corrosion Science.* 1998; 40:2023-2027.

25. Subba Rao R, Wolff U, Baunack S, Eckert J, Gebert A. Corrosion behaviour of the amorphous $Mg_{65}Y_{10}Cu_{15}Ag_{10}$. *Corrosion Science*. 2003; 45:817-832.